The Presence of the WGD Motif in CC8 Heterodimeric Disintegrin Increases Its Inhibitory Effect on αIIbβ3, αvβ3, and α5β1 Integrins†

Juan J. Calvete,‡ Jay W. Fox,§ Alexis Agelan,|| Stefan Niewiarowski,|| and Cezary Marcinkiewicz*,||

Instituto de Biomedicina de Valencia, CSIC, Valencia 46010, Spain, Department of Microbiology, University of Virginia Health Sciences Center, Charlottesville, Virginia 22908, and Sol Sherry Thrombosis Research Center, Department of Microbiology, School of Medicine, Temple University, Philadelphia, Pennsylvania 19140

Received August 1, 2001; Revised Manuscript Received November 27, 2001

ABSTRACT: Two highly homologous dimeric disintegrins, CC5 and CC8, have been isolated from the venom of the North African sand viper *Cerastes cerastes*. CC5 is a homodimer containing an RGD motif in its subunits. CC8 is a heterodimer. The CC8A and CC8B subunits contain RGD and WGD tripeptide sequence in their respective integrin-binding loops. Both CC5 and CC8 inhibited platelet aggregation and the adhesion of cells expressing integrins αIIbβ3, αvβ3, and α5β1 to appropriate ligands. However, the inhibitory activity of CC8 was at least 1 order of magnitude higher than that of CC5. Enhanced activity of CC8 over CC5 was also observed in the induction of LIBS epitopes on β1 and β3 integrins. Synthetic peptides in which the arginyl residue of the RGD motif had been replaced with tryptophans exhibited increased inhibitory activity toward integrins α5β1, αIIbβ3, and αvβ3. Moreover, alanine substitution of the aspartic acid of the WGD motif of these peptides decreased their inhibitory ability, whereas the same substitution in the RGD sequence almost completely abolished the activity of the peptides. We conclude that the WGD motif enhances the inhibitory activity of disintegrins toward αIIbβ3, αvβ3, and α5β1 integrins.

Integrins represent a large family of heterodimeric transmembrane receptors that mediate cell adhesion to extracellular matrix proteins, and cell−cell interactions by adhesive ligands. Integrin receptors are involved in fundamental physiological cellular processes and contribute to the pathology of certain diseases, including tumor metastasis, immune dysfunctions, viral infections, osteoporosis, and coagulopathies (*1*−*3*). At present, 8 β and 18 α subunits have been characterized. These subunits combine in a restricted manner to form at least 24 heterodimers, each exhibiting a distinct ligand binding profile (*3*). A common feature of most of the ligands of integrins αIIbβ3, αvβ3, and α5β1 is the presence of the arginine-glycine-aspartate tripeptide sequence (RGD motif) in their integrin-binding sites. Integrin αIIbβ3 is the fibrinogen receptor, which is expressed on platelets and mediates platelet aggregation in hemostasis and thrombosis (*4*). The αvβ3 integrin, the major vitronectin receptor, is predominantly expressed on endothelial cells and plays pivotal roles in angiogenesis, inflammation, bone resorption, and wound healing. The fibronectin receptor, integrin α5β1, is widely distributed. It is essential for cell growth and organ development. Both α5 (*5*) and β1 (*6*, *7*) null mice show early embryonic lethality. In contrast, αv null mice survive until late stages of embryonic development and occasionally until birth (*8*). On the other hand, β3 null mice develop relatively normally, although they exhibit placental defects (*9*) and abnormalities in osteoclast function (*10*).

Central to the understanding of integrin function in physiology and pathology is an understanding of the basis of ligand recognition and the identification of novel and high-affinity ligands that can be used as lead compounds for specific drug development. Disintegrins, a family of peptides occurring in *Crotalidae* and *Viperidae* snake venoms, are among the most potent antagonists of several integrins (*11*−*13*). Disintegrins are the product of proteolysis of larger mosaic precursors of the PII class of snake venom metalloproteinases (*14*, *15*). The majority of the more than 30 different disintegrins that have been isolated are single-chain polypeptides, which express the RGD motif in their active sites and strongly inhibit αIIbβ3 integrin binding to fibrinogen. Exceptions are barbuorin, which contains the KGD motif (*16*), and atrolysin E/D, which contains a MVD motif (*17*). The KGD sequence confers a high degree of selectivity toward integrin αIIbβ3, whereas atrolysin E/D inhibits ADP- and collagen-induced platelet aggregation.

Dimeric disintegrins represent a newly characterized disintegrin family. Homodimeric disintegrins contain either 10 [contortrostatin (*18*, *19*); CC5 (this work)] or 15 [bilitoxin-1 (*20*)] cysteine residues in their subunits. The integrin-binding motifs of contortrostatin and CC5 contain the RGD sequence, whereas bilitoxin-1 displays an MGD motif. Heterodimeric disintegrins exhibit more variability in their active site sequences than homodimeric disintegrins. EC3, a heterodimeric disintegrin from *Echis carinatus* venom,

† This work was supported by Grants PB98-0694 and BCM2001-3337 from the Ministerio de Ciencia y Tecnologia, Madrid, Spain (to J.J.C.), a Grant-in-Aid from the American Heart Association (to S.N.), and the W. W. Smith Charitable Trust (to C.M.).

* To whom correspondence should be addressed: Sol Sherry Thrombosis Research Center, School of Medicine, Temple University, 3400 N. Broad St., Philadelphia, PA 19140. E-mail: cmarcink@nimbus.temple.edu.

‡ CSIC.

§ University of Virginia Health Sciences Center.

|| Temple University.

10.1021/bi015627o CCC: $22.00
Published on Web 01/17/2002

contains a VGD motif in its A-subunit and the MLD tripeptide in the B-subunit (*21*). It is a selective and potent inhibitor of the binding of α4β1 and α4β7 integrins to immobilized VCAM-1 and MAdCAM-1, respectively (*21*). It also potently inhibits α9β1 integrin binding to VCAM-1, but not to osteopontin and tenascin-C (*22*). EC3 is a weak inhibitor of α5β1 and αIIbβ3 integrins, and shows no inhibition of the αvβ3 integrins. The inhibitory activity of EC3 toward the α4β1 and α9β1 integrins has been associated with the MLD sequence of the B-subunit, whereas both the EC3A and EC3B subunits possess α5β1 inhibitory activity. EC6, another heterodimeric disintegrin isolated from *E. carinatus* venom (*22*), exhibited effects on α4 and α9β1 integrins very similar to those of EC3 due to the presence of the MLD sequence in the A-subunit. The EC6B subunit contains the RGD sequence and acts as a potent antagonist of the α5β1 integrin. EMF10, a heterodimeric disintegrin isolated from the venom of *Eristocophis macmahoni*, is a potent and selective inhibitor of integrin α5β1 binding to fibronectin and a weak inhibitor of αIIbβ3, αvβ3, and α4β1 integrins (*23*). Selective recognition of α5β1 integrin by EMF10 has been mapped to both the MGD(W) sequence within the active loop of the B-subunit and the RGD(N) motif of the A-subunit. Here, we report the structural and biochemical characterization of novel heterodimeric disintegrins CC5 and CC8. The novel WGD motif in the integrin binding loop of the B-subunit of CC8 endows the disintegrin with enhanced inhibitory activity toward αIIbβ3, αvβ3, and α5β1 integrins.

EXPERIMENTAL PROCEDURES

Materials. Monoclonal antibody Mab62, specific for epitope LIBS2 in the C-terminal region of the extracellular domain of the β3 subunit (*24*), was provided by M. Ginsberg (Scripps Research Institute, La Jolla, CA). The monoclonal antibody 9EG7 that recognizes an LIBS epitope on β1 integrin (*25*) was purchased from Pharmingen (San Diego, CA). Highly purified fibrinogen was a gift from A. Budzynski (Temple University). Human fibronectin and human vitronectin were purchased from Sigma (St. Louis, MO) and Chemicon (Temecula, CA).

Cell Lines. A5 cells, Chinese hamster ovary (CHO) cells transfected with human αIIbβ3 integrin (*26*), were kindly provided by M. Ginsberg (Scripps Research Institute). JY cells expressing αvβ3 were a gift from Dr. Burakoff (Dana Farber Cancer Institute, Boston, MA). K562 cells and CHO K1 cells were purchased from ATCC (Manassas, VA).

Purification of Dimeric Disintegrins. Lyophilized venom from *Cerastes cerastes*, purchased from Latoxan Serpentarium (Rosans, France), was dissolved at 30 mg/mL in 0.1% trifluoroacetic acid. Insoluble material was discarded after centrifugation at 5000 rpm for 5 min, and the supernatant was fractionated by reverse-phase HPLC on a Vydac (Hesperia, CA) C18 column (250 mm × 10 mm). The column was eluted with a linear 0 to 80% acetonitrile gradient over the course of 45 min at a flow rate of 2 mL/min. Separations were monitored at 206 nm. Fractions were collected manually, and lyophilized using a Speed-Vac system. HPLC fractions were denoted CC*n* (where *n* is the fraction number in order of elution). Lyophilized fractions were dissolved in water, and the protein concentration was determined using the BCA assay (Pierce, Rockford, IL). Fractions containing 5 μg of total protein in PBS were immobilized overnight at 4 °C on 96-well microtiter plates (Falcon, Pittsburgh, PA), and tested for their ability to support adhesion of K562 cells (as described below). Fractions with adhesive properties were tested for their inhibitory effect on adhesion of K562 cells to immobilized fibronectin. Active fractions (CC5 and CC8) were rechromatographed using the same reverse-phase HPLC system but developing the column with a 0 to 60% acetonitrile gradient over the course of 45 min. The main HPLC peaks displaying an inhibitory effect on adhesion of K562 cells to fibronectin were lyophilized. The purity of isolated dimeric disintegrins was assessed by SDS−polyacrylamide gel electrophoresis and matrix-assisted laser desoption ionization time-of-flight mass spectrometry (MALDI-TOF-MS) performed at the Wistar Mass Spectrometry Facility (Philadelphia, PA) using a PE-Biosystems Voyager-DE Pro instrument.

Isolation and Structural Characterization of Ethylpyridylated Subunits. CC5 and CC8 proteins [0.5 mg/mL in 0.1 M Tris-HCl (pH 8.5), 4 mM EDTA, and 6 M guanidine hydrochloride] were reduced with 3.2 mM dithiothreitol for 2 h at room temperature in the dark. Reduced proteins were alkylated by addition of a 2-fold molar excess of 4-vinylpyridine over a reducing reagent. Ethylpyridylated (EP) subunits were isolated by reverse-phase HPLC on a C18 column developed with a linear gradient of 0.1% TFA in water (solution A) and 0.1% TFA in acetonitrile (solution B), and were denoted "A" or "B" according to their elution order. The isolated EP subunits were initially characterized by N-terminal sequencing (using either an Applied Biosystems 477A or a Beckman Porton LF-3000 instrument following the manufacturer's instructions), amino acid analysis (using a Beckman Gold Amino Acid Analyzer after sample hydrolysis in 6 M HCl for 24 h in evacuated and sealed ampules), and MALDI-TOF mass spectrometry (as above). The primary structures of EP polypeptides were deduced from N-terminal sequence analysis of overlapping peptides obtained by proteolytic digestions with TPCK-trypsin (Sigma), endoproteinases Lys-C (Boehringer Mannheim), and endoproteinase Asp-N (Boehringer Mannheim) [2 mg/mL protein in 100 mM ammonium bicarbonate (pH 8.3) for 18 h at 37 °C using an enzyme:substrate ratio of 1:100 (w/w)] and degradation with CNBr [10 mg/mL protein and 100 mg/mL CNBr in 70% (v/v) formic acid for 6 h at room temperature, under an N_2 atmosphere in the dark]. Peptides were separated by reverse-phase HPLC using a 4 mm × 250 mm C18 (5 μm particle size) Lichrospher RP100 (Merck) column eluting at 1 mL/min with a linear gradient of 0.1% TFA in water (solution A) and 0.1% TFA in acetonitrile (solution B).

Peptide Synthesis. Peptides LPAWGDFDNDL (CC8B 39−49), LPAWGAFDNDL (CC8B 39−49 D44A), WGDF (CC8B 42−45), and WGAF (CC8B 42−45 D44A) were synthesized on a Symphony multiple-peptide synthesizer (Rainin) using Fmoc [*N*-(9-fluorenyl)methoxycarbonyl] chemistry as suggested by the manufacturer. Peptide amide linker resin with 0.37 mmol/g substitution (Perseptive Biosystems) was used as the solid support. Cleavage and deprotection of the peptides were performed on the synthesizer using 88% trifluoroacetic acid, 2% diisopropylsilane, 5% water, and 5% phenol. Following cleavage, the ether-extracted crude peptide product was desalted and purified on a preparative C18

reverse-phase column (250 mm × 21.4 mm, Rainin) using a 0.1% trifluoroacetic acid/water solution with a gradient in acetonitrile (from 5 to 80%). The purity of the peptides was assessed by analytical reverse-phase high-performance liquid chromatography and MALDI-TOF mass spectrometry.

Cell Adhesion Studies. Adhesion studies of cultured cells labeled with 5-(chloromethyl)fluorescein diacetate (CMFDA) were performed as described previously (*27*). Briefly, disintegrins, fibrinogen, fibronectin, vitronectin, or anti-LIBS monoclonal antibodies were immobilized on a 96-well microtiter plate (Falcon) in PBS buffer overnight at 4 °C. Wells were blocked with 1% BSA[1] in Hank's balanced salt solution (HBSS) containing calcium and magnesium. The cells were labeled with fluorescein by incubation at 37 °C for 15 min with 12.5 μM CMFDA in HBSS containing calcium and magnesium. Cells were freed from unbound ligand by washing with the same buffer. Labeled cells (1×10^5/sample) were added to the wells in the presence or absence of inhibitors and incubated at 37 °C for 30 min. Unbound cells were removed by aspiration; the wells were washed, and bound cells were lysed by adding 0.5% Triton X-100. In parallel, the standard curve was prepared in the same plate using known concentrations of labeled cells. The plates were read using a Cytofluor 2350 fluorescence plate reader (Millipore, Bedford, MA) at an excitation wavelength of 485 nm using a 530 nm emission filter.

Platelet Aggregation Assay. A platelet aggregation assay was performed using platelet rich plasma (PRP) isolated from human blood in the presence of 0.4% sodium citrate as described previously (*27*).

RESULTS

Localization and Purification of Disintegrins with Anti-α5β1 Activity from C. cerases Venom. Reverse-phase HPLC fractionation of soluble proteins of the venom of *C. cerastes* yielded 17 fractions (Figure 1A). Each fraction was analyzed for its ability to support binding of K562 cells expressing α5β1 integrin. Fractions CC4−CC17 exhibited this binding activity, albeit with different avidities. The highest adhesion activity was found in the CC8 fraction followed by CC5 and CC9 (data not shown). Fractions with K562 adhesive activity were further tested for inhibition of adhesion of K562 cells to immobilized fibronectin mediated by α5β1 integrin. The strongest inhibitory activities were found with fractions CC5 and CC8 (Figure 1B). These two fractions were subjected to purification of α5β1 integrin inhibitors, using the second step of reverse-phase HPLC as described in Experimental Procedures. The purity of the isolated dimeric disintegrins was assessed by mass spectrometry and SDS−PAGE. The yields of purified CC5 and CC8 were ∼4 and ∼12 mg of protein from 1 g of crude venom, respectively.

Subunit Composition of CC5 and CC8. Mass spectrometric analysis of native CC5 yielded two isotope-averaged molecular ions of 14 052 ± 2 and 14 184 ± 2 Da. CC8 also

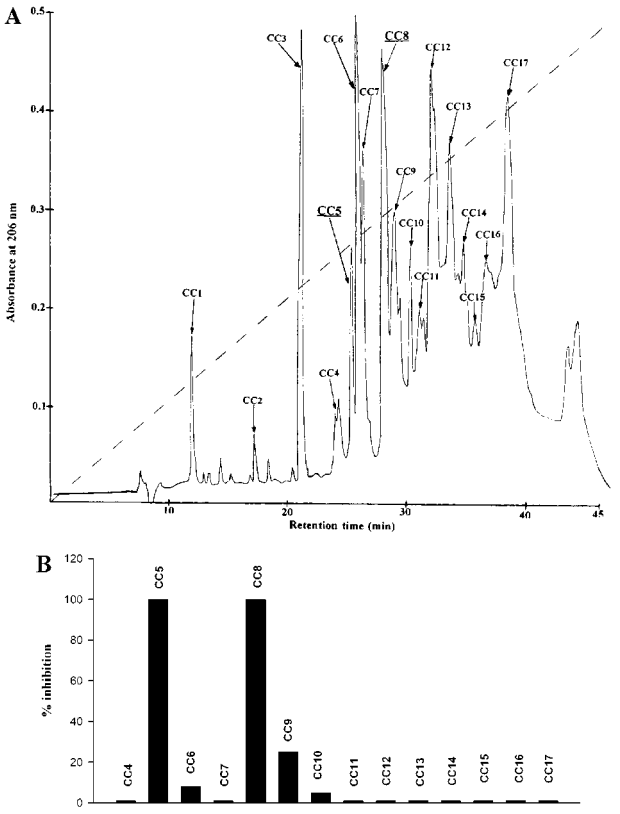

FIGURE 1: Localization of fractions within *C. cerastes* viper venom with an inhibitory effect on α5β1 integrin interaction with fibronectin. (A) Fractionation of the venom on reverse-phase HPLC. The crude venom was dissolved in 0.1% TFA and injected (10 mg in 400 μL) in a C18 column. Fractions separated with an 0 to 80% acetonitrile gradient (− − −) were collected and lyophilized. (B) Inhibition of K562 cell adhesion to immobilized fibronectin. CC fractions with adhesive properties were tested for their ability to inhibit K562 cell adhesion to immobilized fibronectin (1 μg per well). Five micrograms of each CC fraction (from CC4 to CC17) was incubated for 30 min at 37 °C on the 96-well plate with immobilized fibronectin in the presence of CMFDA-labeled K562 cells. After being washed, the bound cells were lysed with Triton X-100, and the fluorescence intensity was determined as described above. The percent inhibition of CC fractions was calculated by comparison with the fluorescence of control samples without inhibitors.

exhibited two molecular ions at *m*/*z* 14 150 ± 2 and 14 019 ± 2. After reduction and alkylation with vinylpyridine, both CC5 and CC8 were separated into two subunits by reverse-phase HPLC, termed subunit A and subunit B, respectively. Ethylpyridylated (EP) CC5A exhibited two isotope-averaged molecular ions of 8229 ± 1 and 8098 ± 1 Da, while EP CC5B yielded a single ion of 8098 ± 1 Da. On the other hand, the mass spectrum of EP CC8A exhibited two ions of 8238 ± 2 and 8107 ± 2 Da, and that of EP CC8B displayed a single ion at 8078 ± 1 Da. N-Terminal sequence analysis of CC5 showed that the protein consisted of a mixture of two polypeptides, EP CC5A1 (MNSAHPCCDPVTCKPKRGEHCIS) and EP CC5A2 (NSAHPCCDPVTCKPKRGEHCISG), with identical amino acid sequences except that the N-terminal methionine residue of EP CC5A1 was missing in EP CC5A2. The N-terminal sequence of EP CC5B was identical to that of EP CC5A2. These sequences share a high degree of similarity with the subunits of other dimeric disintegrins (see below). In addition, the data clearly indicated that CC5 was a mixture of two dimeric proteins, CC5.1 with

[1] Abbreviations: BSA, bovine serum albumin; CMFDA, 5-(chloromethyl)fluorescein diacetate; HBSS, Hank's balanced salt solution; HPLC, high-performance liquid chromatography; LIBS, ligand-induced binding site; MALDI-TOF-MS, matrix-assisted laser desoption ionization time-of-flight mass spectrometry; MAdCAM-1, mucosal addressin cell adhesion molecule 1; PBS, phosphate-buffered saline; PRP, platelet rich plasma; TFA, trifluoroacetic acid; VCAM-1, vascular cell adhesion molecule 1.

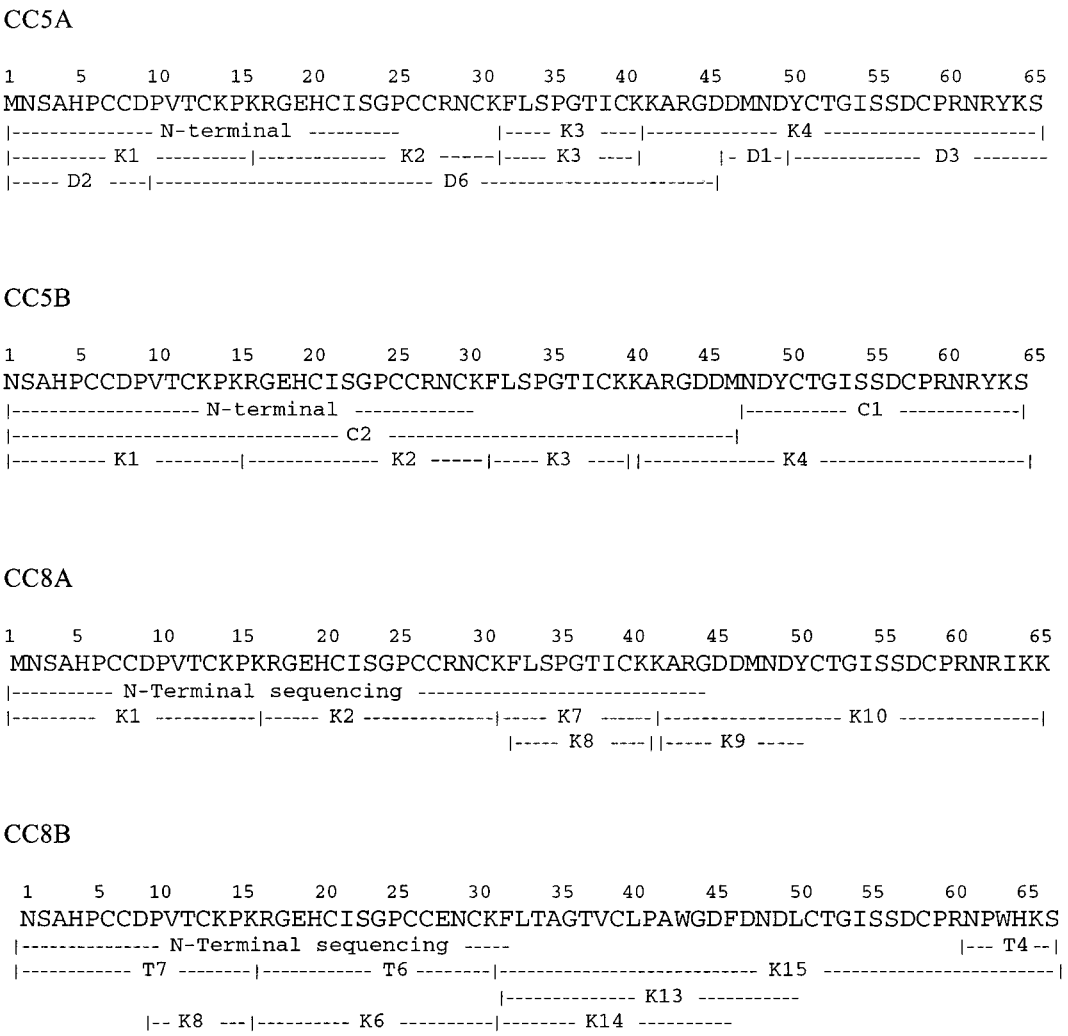

FIGURE 2: Amino acid sequences of CC5 and CC8 subunits. The amino acid sequences of CC5A, CC5B, CC8A, and CC8B were established by automated Edman degradation of reduced and ethylpyridylated subunits, and by N-terminal sequencing of overlapping peptides isolated by reverse-phase HPLC after degradation of the polypeptides with endoproteinase Lys-C (K) and Asp-N (D), trypsin (T), and cyanogen bromide (CNBr).

a CC5A1−CC5A2 or CC5A1−CC5B subunit composition and CC5.2, a homodimer of CC5A2 subunits or a CC5A2−CC5B heterodimer. Amino acid analysis of iodoacetamide-treated CC5 showed that it did not contain free sulfhydryl groups. On the other hand, amino acid analysis of EP CC5A and EP CC5B indicated that each CC5 subunit contained 10 cysteine residues per molecule.

Like that of EP CC5A, N-terminal sequence analysis of EP CC8A also exhibited a mixture of two sequences differing in the presence or absence of an N-terminal methionine residue and in the residue at position 28 of the longer polypeptide (underlined): EP CC8A1 (MNSAHPCCDPVTCKPKRGEHCISGPCCRNCKFL) and EP CC8A2 (NSAHPCCDPVTCKPKRGEHCISGPCCENCKFL). The N-terminal sequence of EP CC8B was identical to that of EP CC8A1 except for the absence of the N-terminal methionine residue. CC8 did not contain sulfhydryl groups, and 10 cysteine residues/molecule were quantitated in each EP CC8 chain by amino acid analysis. Hence, like CC5, CC8 contained a mixture of two heterodimeric disintegrins with CC8A1−CC8B and CC8A2−CC8B subunit compositions.

Amino Acid Sequences of CC5 and CC8. The complete amino acid sequences of the ethylpyridylated CC5 and CC8 subunits were determined by N-terminal sequence analysis of reverse-phase HPLC-isolated peptides derived by degradation of each subunit with TPCK-trypsin, endoproteinases Lys-C and Asp-N, and cyanogen bromide (Figure 2). The primary structures of CC5A and CC5B are identical, except for the presence of an extra N-terminal methionine residue in the A-subunit. The calculated isotope-averaged molecular masses for CC5A and CC5B are 7159.3 and 7028.3 Da, respectively. The calculated molecular mass of native CC5.1 (7159.3 + 7028.3 − 20) is 14 167.6 Da, and that of CC5.2 (7028.3 + 7028.3 − 20) is 14 036.6 Da. The mass difference of ∼16 Da between the experimental masses of CC5 (14 184 and 14 052 Da) and the masses calculated for CC5.1 and CC5.2 from subunit combinations suggested that a methionine residue was oxidized to the sulfoxide derivative during isolation of CC5.

The amino acid sequence of CC8A is identical to that of CC5A/B, except for the C-terminal residue (Figure 2). The primary structure of CC8B also shares a large degree of sequence identity with CC5A/B and CC8A polypeptides differing essentially in the region encompassing residues 33−49. The calculated isotope-averaged molecular masses for CC8A and CC8B are 7143.3 and 7026.1 Da, respectively.

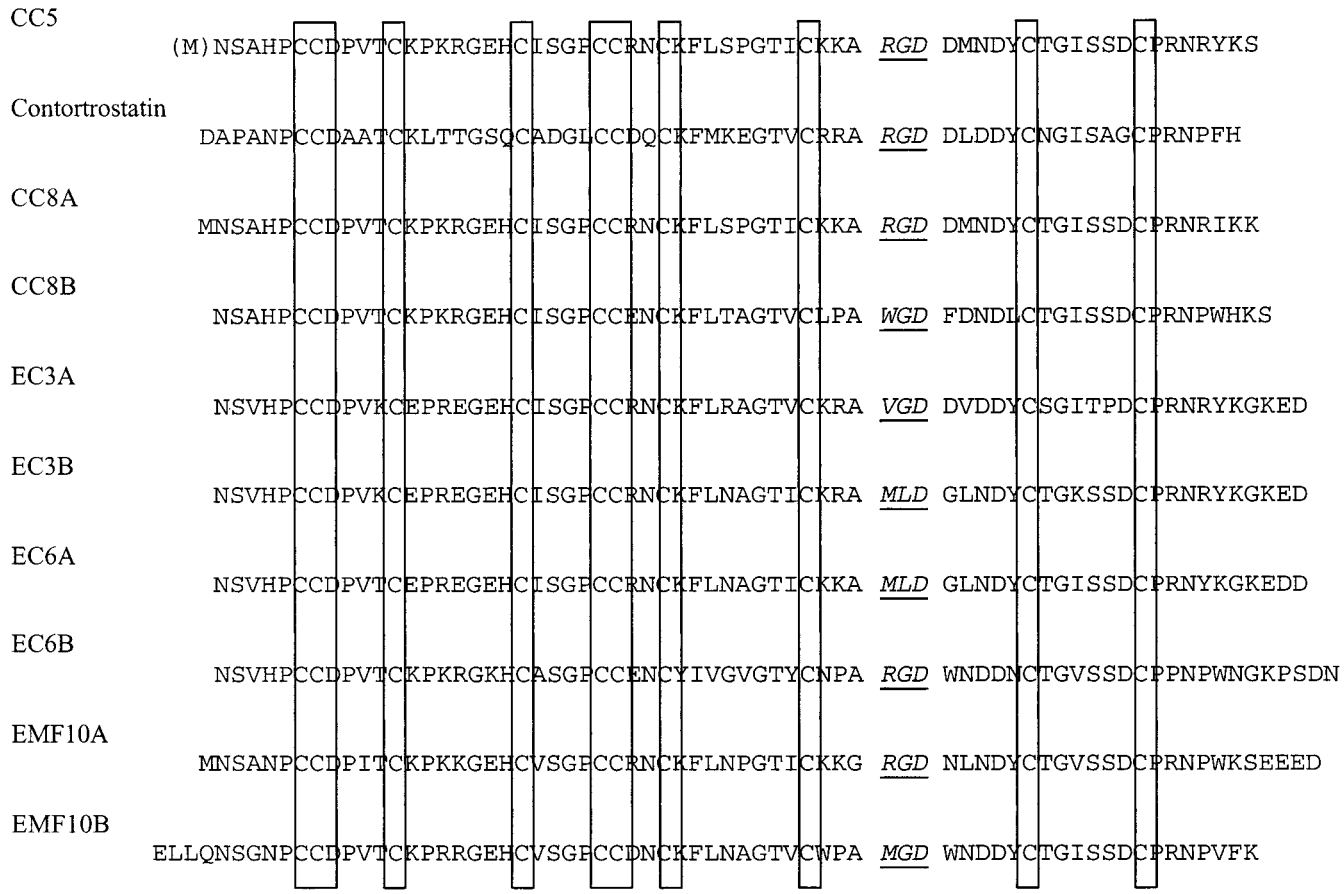

FIGURE 3: Comparison of amino acid sequences of CC5 and CC8 with other dimeric disinetgrins. CC5 and contortrostatin (*16*) represent homodimeric disintegrins; CC8, EC3 (*18*), EC6 (*19*), and EMF10 (*20*) represent heterodimeric disintegrins. Cysteine residues are boxed. The integrin-binding motifs are indicated in italics and underlined.

These data established that CC8 is a mixture of two heterodimers, CC8.1 (14 150 ± 2 Da) and CC8.2 (14 019 ± 2 Da), composed of a common B-subunit disulfide linked to either CC8A1 or CC8A2. The calculated isotope-averaged molecular masses of CC8.1 (7143 + 7028 − 20) and CC8.2 (7012 + 7028 − 20) are 14 151 and 14 020 Da, respectively, which are in excellent agreement with the experimentally determined MALDI-TOF masses. On the other hand, the mass difference of 40 Da between the MALDI-TOF masses of the native CC8 proteins and the masses calculated from ethylpyridylated subunit mass information {CC8.1 [8238 + 8078 − (20 × 106.3)], 14 190 Da; CC8.2 [8107 + 8078 − (20 × 106.3), 14059 Da} suggested that modification took place during subunit preparation.

The sequences of the primary structures of the CC5 and CC8 dimeric disintegrins isolated from venom of *C. cerases* sand viper are very similar to the sequences of other dimeric disintegrins (Figure 3). The most characteristic feature for this family of proteins is the presence of 10 cysteines in each subunit. Moreover, homodimeric disintegrins (contortrostatin, CC5) contain the RGD sequence in their active site, while hetrodimeric disintegrins show more variability in this site. EC3 has VGD and MLD motifs. EC6 has MLD and RGD motifs. EMF10 has RGD and MGD motifs. CC8 has RGD and WGD motifs.

Biological Activities of CC5 and CC8. The inhibitory activity of CC5 and CC8 against RGD-dependent integrins has been tested in a cell adhesion assay (Figure 4). In each system, CC8 was at least 1 order of magnitude more potent then CC5 in the inhibition of cell adhesion to the appropriate, immobilized ligand. In K562 cell adhesion to immobilized fibronectin, CC5 displayed an IC_{50} of 3.5 nM, whereas the IC_{50} of CC8 was 0.5 nM (Figure 4A). CC5 and CC8 inhibited the adhesion of A5 cells to immobilized fibrinogen with IC_{50} values of 63 and 2 nM, respectively (Figure 4B). CC8 was also much more potent than CC5 in blocking the adhesion of JY cells to immobilized vitronectin (IC_{50} = 12 vs 42 pM) (Figure 4C). The higher antagonistic effect of CC8 toward integrin αIIbβ3 was confirmed in an ADP-induced platelet aggregation assay. CC5 and CC8 inhibited platelet aggregation with IC_{50} values of 93 and 11 nM, respectively. In other β1 integrin systems, such as α1β1, α2β1, α4β1, and α6β1, CC5 did not show any inhibitory effect when added up to a final concentration of 5 μM (data not shown). CC8 had similar properties except for adhesion Jurkat cells (expressing α4β1 integrin) to immobilized recombinant VCAM-1. In this adhesion system, CC8 exhibited an inhibitory effect with an IC_{50} of 300 nM (data not shown).

Expression of LIBS mediated by CC5 and CC8 was tested in an adhesion assay measuring the number of cells adhered to immobilized anti-LIBS monoclonal antibodies in the presence of disintegrins. CC8 was a potent LIBS inducer in both β1 (Figure 5A) and β3 (Figure 5B) integrins. The level of LIBS expression caused by CC5 was at least 10 000 cells lower at the point of saturation.

Activity of Synthetic Peptides Containing the WGD Sequence. The inhibitory effect of CC8B-derived peptides was assessed in adhesion systems of cells expressing RGD-

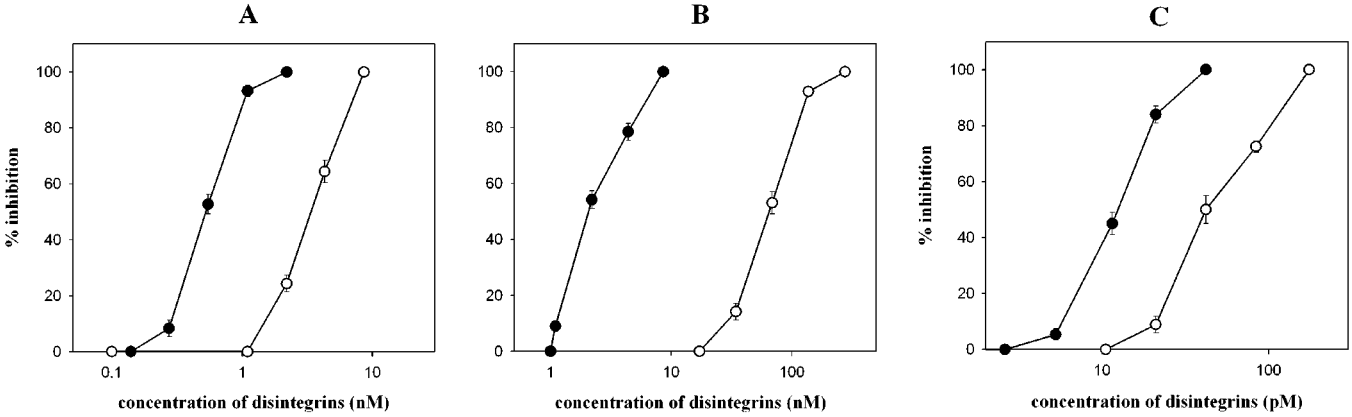

FIGURE 4: Comparison of cell adhesion inhibitory activities of CC5 (○) and CC8 (●) on the adhesion of K562 cells to immobilized fibronectin (A), A5 cells to immobilized fibrinogen (B), and JY cells to immobilized vitronectin (C) was tested using CMFDA-labeled cells. Different concentrations of disintegrins were incubated (30 min at 37 °C) with the cells (1×10^5) in the 96-well plate covered with the appropriate ligand, in 100 μL of HBSS containing calcium and magnesium. After being washed with the same buffer, the adhered cells were lysed with Triton X-100, and the plate was read using Cytofluor 2350. Percent inhibition was calculated by comparison with the fluorescence obtained from control sample without disintegrins. The error bars represent the standard deviation from three independent experiments.

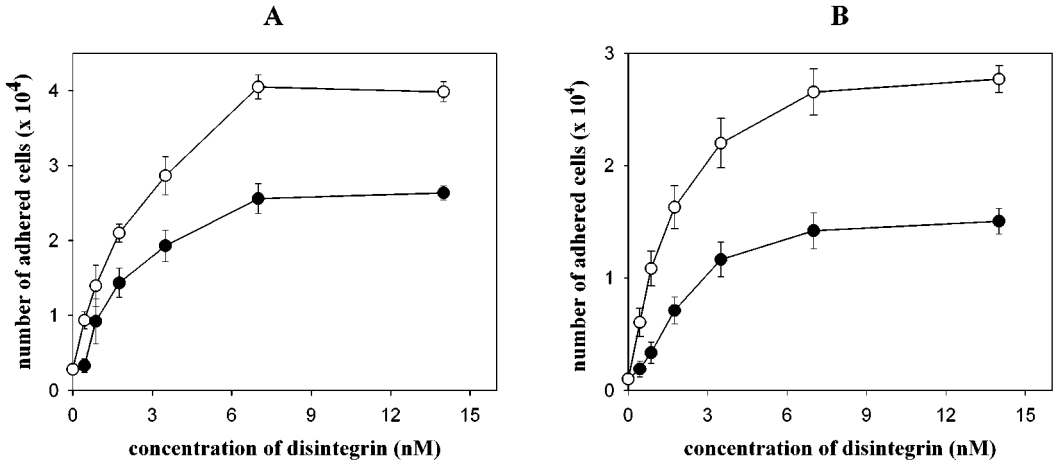

FIGURE 5: Effect of CC5 and CC8 on LIBS expression. The ability to trigger LIBS expression was assessed for CC5 (●) and CC8 (○) in the assay of adhesion of K562 cells to immobilized 9EG7 monoclonal antibody (A) and A5 cells to the immobilized Mab62 monoclonal antibody (B). 9EG7 recognizes the LIBS epitope on the β1 subunit of $\alpha 5\beta 1$ integrin, and Mab62 binds to the LIBS epitope on the β3 subunit of $\alpha IIb\beta 3$ integrin. The antibodies (1 μg per sample in PBS) were immobilized in 96-well plates overnight at 4 °C. The CMFDA-labeled cells were added to the wells in the presence or absence of disintegrins, and the number of adhered cells was determined as described in the legend of Figure 1B. The error bars represent standard deviations from three experiments.

dependent integrins to their ligands (Figure 6). Two peptides were designed on the basis of the amino acid sequence of the putative integrin-binding region of CC8B: the Ac-LPAWGDFDNDL-NH_2 peptide, which represents the entire integrin-binding loop, and the Ac-WGDF-NH_2 tetrapeptide, which is topologically equivalent of the active motifs of other disintegrins, such as the RGDD motif in echistatin (*28*), the RGDW motif in eristostatin (*29*), the MGDW motif in EMF10 (*23*), or the MLDG motif in EC3 and EC6 (*21*, *22*). Both peptides had very similar blocking activities ($IC_{50} \sim 1$ mM) on of the adhesion of (i) K562 cells to fibronectin (Figure 6A), (ii) A5 cells to fibrinogen (Figure 6B), and (iii) JY cells to vitronectin (Figure 6C). Furthermore, in contrast to previous studies using RGD-containing peptides showing the critical importance of the aspartic acid for expression of integrin inhibitory activity, substitution of the aspartic acid of the WGD sequence with alanine decreased, but did not completely abolish, the inhibitory activities of the peptides (Figure 6).

Table 1 shows the effect on inhibition of RGD-dependent integrins of synthetic peptides containing the WGD motif. In each adhesion system, the inhibitory activity of the WGDF peptide was at least 2-fold greater than that of the RGDF peptide. Moreover, replacement of aspartic acid of the WGDF peptide with alanine increased the IC_{50} 3−4-fold, whereas the same substitution in the RGDF peptide abolished its inhibitory activity ($IC_{50} > 20$ mM).

The inhibitory effect of CC8 and of the synthetic WGDF peptide on cell adhesion assays mediated by RGD-dependent integrins $\alpha 5\beta 1$, $\alpha IIb\beta 3$, and $\alpha v\beta 3$ did not change in the presence of either 1 mM Ca^{2+}, Mg^{2+}, or Mn^{2+}.

DISCUSSION

We report the characterization of two new dimeric disintegrins, CC5 and CC8, isolated by reverse-phase HPLC from the venom of the North Africa sand viper *C. cerastes* (Figure 1A). It is worth noting that whereas medium-size monomeric disintegrins have been found only in *Crotalidae*

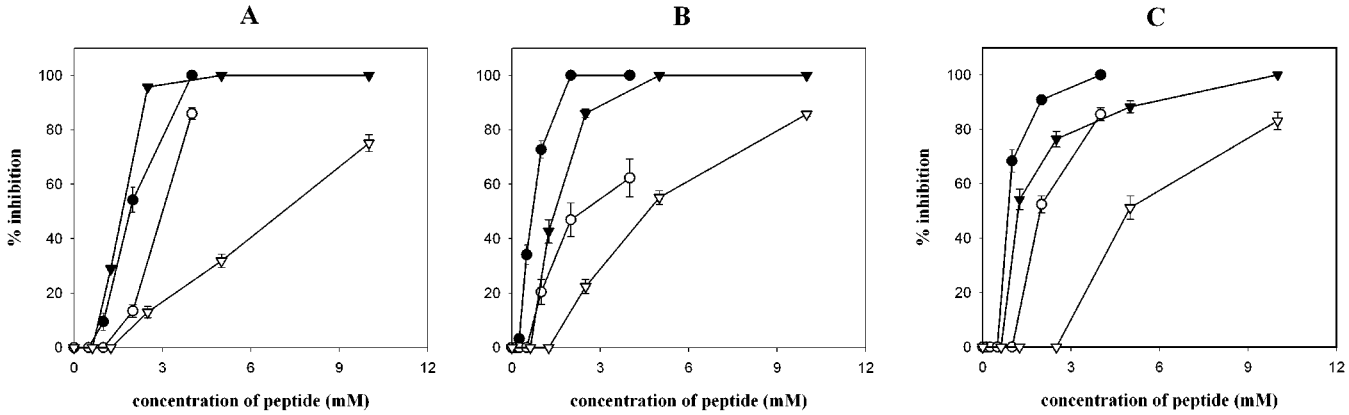

FIGURE 6: Effect of synthetic peptides, designed on the basis of the active site of CC8B, on cell adhesion. The inhibitory effect of synthetic peptides LPAWGDFDNDL [representing the entire integrin-binding loop (●)] and WGDF [representing the integrin-binding motif (▼)] and the corresponding control peptides LPAWGAFLDNDL (○) and WGAF (▽) on the adhesion of K562 cells to immobilized fibronectin (A), A5 cells to immobilized fibrinogen (B), and JY cells to immobilized vitronectin (C) was tested with CMFDA-labeled cells as described in the legend of Figure 4. Error bars represent standard deviations from three experiments.

Table 1: Effect of Synthetic Peptides on Cell Adhesion to RGD-Containing Ligands[a]

peptide cell line/ligand	WGDF	WGAF	RGDF	RGAF
K562/FN	1.65	7.26	3.64	>10
A5/FG	1.45	5.20	2.96	>10
JY/VN	1.28	4.96	2.84	>10

[a] The experiments were performed in assays of adhesion of three cell lines to the appropriate ligand. The data represent IC_{50}s (millimolar) calculated as means from three independent experiments. Cells: K562, cells expressing $\alpha5\beta1$; A5, cells expressing $\alpha IIb\beta3$; JY, cells expressing $\alpha v\beta3$. Ligands: FN, fibronectin; FG, fibrinogen; VN, vitronectin. The data represent means from three independent experiments.

vipers, and long and short monomeric disintegrins appear to be restricted to venoms of *Viperidae* snakes, dimeric disintegrins have been isolated from venoms of snakes belonging to both genera: CC5 and CC8 from *C. cerastes* (this work), lebein (*30*), VLO4 and VLO5 from *Vipera lebetina obtusa*, and VB7 from *Vipera berus* (unpublished observations) and EC3 and EC6 from *E. carinatus* (*21*, *22*) and EMF10 from *Eristocophis macmahoni* (*23*, *31*) and *Crotalidae* [contortrostatin from *Agkistrodon contortrix contortrix* (*19*, *32*, *33*) and piscivostatin from *Agkistrodon piscivorus piscivorus* (*34*)].

CC5 and CC8 exhibited strong inhibitory activity on the adhesion of K562 cells to immobilized fibronectin (Figure 1B). CC5 is a dimer, the subunit primary structures of which differ only in the presence (CC5A) or absence (CC5B) of an N-terminal methionine residue. CC8 is a heterodimer of structurally related subunits. Moreover, CC8A has an amino acid sequence identical to that of the CC5 subunits, except for the C-terminal residue (Figure 2). Like all dimeric disintegrins characterized to date, except billitoxin (*20*), the CC5 and CC8 subunits contain 10 cysteine residues. Like the homodimeric disintegrin contortrostatin (*33*) and lebein (*30*), both CC5 subunits express RGD motifs in their integrin-binding loops and potently interact with RGD-dependent integrins. Although the integrin-binding loops of the CC5 and CC8A subunits closely resemble that of contortrostatin (Figure 3), there are no data available comparing their inhibitory activities toward RGD-dependent integrins. However, contortrostatin contains leucine (^{43}RGDDL^{47}) at position 47, which is methionine in CC5/CC8A (Figure 3), and previous studies with recombinant mutants of echistatin (*29*) revealed that replacement of methionine with leucine within the RGDDM sequence inhibited the ability of echistatin to recognize $\alpha5\beta1$ integrin.

Dimeric disintegrins display more variability in their active site motifs than any other group of the disintegrin family. For example, the tripeptide motifs RGD (EC6B, EMF10A, and CC8A), MLD (EC3B and EC6A), MGD (EMF10B), and VGD (EC3A) have been reported (Figure 3). We now add the WGD motif found in CC8B to this growing list. The arginine to tryptophan substitution appears to endow CC8 with the strongest reported inhibitory activity toward $\alpha IIb\beta3$, $\alpha v\beta3$, and $\alpha5\beta1$ integrins. Compared with CC5, CC8 is a better inhibitor of these three RGD-dependent integrins by at least 1 order of magnitude (Figure 4). Particularly impressive is the potent inhibitory effect of CC8 on ADP-induced platelet aggregation ($IC_{50} = 2$ nM). When injected in mice, CC8 caused severe bleeding and death of the animals (unpublished observations). This deadly effect was most probably caused by the high affinity of binding of CC8 to the platelet fibrinogen receptor, the $\alpha IIb\beta3$ integrin. Previous experiments with disintegrins in animal models never showed such a devastating effect (*35*, *36*). The stronger antagonistic effect of CC8 than of CC5 on $\beta3$ integrins and $\alpha5\beta1$ integrin is also reflected in LIBS expression. As shown in Figure 5, CC8 induced the expression of the epitopes recognized by the LIBS monoclonal antibodies 9EG7 (anti-$\beta1$) (Figure 5A) and Mab62 (anti-$\beta3$) (Figure 5B) in a higher number of cells than CC5. A correlation between the disintegrin inhibitory effect and LIBS expression has also been reported for monomeric disintegrins (*27*, *29*). Moreover, the importance of the C-terminus of disintegrins in LIBS induction has been documented. CC8 and CC5 subunits have distinct C-terminal sequences (PRNRYKS in CC5 subunits and CC8A; PRNPWHKS in CC8B) (Figure 2), which are also different from those of other dimeric disintegrin subunits (Figure 3). The hypothesis that these differences may also affect the potency of LIBS expression is being investigated in our laboratories.

The integrin antagonistic activity of the WGD motif was confirmed using synthetic peptides. Both the LPAWGDFDNDL peptide representing the entire integrin-binding loop of CC8B and the short WGDF peptide (the topologically equivalent of the RGDX motifs from other disintegrins)

showed similar effects on inhibition of the binding of the three RGD-dependent integrins tested to their ligands (Figure 6). Interestingly, although the aspartic acid residue of the RGD and MGD motifs has been shown to be essential for the biological activity of monomeric disintegrins (*37*) and dimeric disintegrin EMF10 (*23*), replacement of the aspartic acid of the WGD sequence with alanine only partially decreased the inhibitory activity of the synthetic peptides. This suggests that structural features of the WGD motif imposed by the tryptophan residue may partially compensate for the absence of the carboxylate site chain of aspartate. More direct evidence of the higher potency of WGD-containing ligands than of RGD-containing ligands in inhibiting RGD-dependent integrins has been assessed by comparing the inhibitory activities of WGDF and RGDF peptides on adhesion of (i) K562 cells to immobilized fibronectin, (ii) A5 cells to fibrinogen, and (iii) JY cells to vitronectin. In each system, the WGDF peptide was at least twice as potent as the RGDF peptide (Table 1). These experiments also confirmed that the tryptophan for arginine replacement partially compensates for the lost activity which results from the alanine substitution of the aspartic acid. Moreover, the activity of the WGD-containing peptides was cation-independent (Ca^{2+}, Mg^{2+}, or Mn^{2+}). In conclusion, the substitution of the RGD motif for the WGD motif resulted in enhanced inhibitory activity of disintegrin CC8 toward integrins $\alpha IIb\beta3$, $\alpha v\beta3$, and $\alpha5\beta1$. This observation may be relevant for the rational design of integrin antagonists with higher affinity toward RGD-dependent integrins (*38*, *39*).

REFERENCES

1. Hynes, R. O. (1992) *Cell 69*, 11−25.
2. Ruoslahti, E. (1996) *Annu. Rev. Cell Dev. Biol. 12*, 697−715.
3. Sheppard, D. (2000) *Matrix Biol. 19*, 203−209.
4. Calvete, J. J. (1999) *Proc. Soc. Exp. Biol. Med. 222*, 29−38.
5. Yang, J. T., Rayburn, H., and Hynes, R. O. (1993) *Development 119*, 1093−1105.
6. Fassler, R., and Mayer, M. (1995) *Genes Dev. 9*, 1896−1908.
7. Stephens, Klimanskaya, I. V., Andrieux, A., Maneses, J., Pedersen, R. A., and Damsky, C. H. (1995) *Genes Dev. 9*, 1883−1895.
8. Bader, B. L., Rayburn, H., Crowley, D., and Hynes, R. O. (1998) *Cell 95*, 5007−5019.
9. Hodivala-Dilke, K. M., McHugh, K. P., Tsakiris, D. A., Raynburn, H., Crowley, D., Ullman-Cullere, M., Ross, F. P., Coller, B. S., Teitelbaum, S., and Hynes, R. O. (1999) *J. Clin. Invest. 103*, 229−238.
10. McHugh, K. P., Hodivala-Dilke, K. M., Zheng, M. H., Namba, N., Lam, J., Novack, D., Feng, X., Ross, F. P., Hynes, R. O., and Teitelbaum, S. L. (2000) *J. Clin. Invest. 105*, 433−440.
11. Dennis, M. S., Henzel, W. J., Pitti, R. M., Lipari, M. T., Napier, M. A., Deisher, T. A., Bunting, S., and Lazarus, R. A. (1990) *Proc. Natl. Acad. Sci. U.S.A. 87*, 2471−2475.
12. Niewiarowski, S., McLane, M. A., Kloczewiak, M., and Stewart, G. J. (1994) *Semin. Hematol. 31*, 289−300.
13. McLane, M. A., Marcinkiewicz, C., Vijay-Kumar, S., Wierzbicka-Patynowski, I., and Niewiarowski, S. (1998) *Proc. Soc. Exp. Biol. Med. 219*, 109−119.
14. Kini, R. M., and Evans, H. J. (1992) *Toxicon 30*, 265−293.
15. Jia, L.-G., Shimokawa, K.-i., Bjarnason, J. B., and Fox, J. W. (1996) *Toxicon 34*, 1269−1276.
16. Scarborough, R. M., Rose, J. W., Hsu, M. A., Phillips, D. R., Fried, V. A., Campbell, A. M., Nannizzi, L., and Charo, I. F. (1991) *J. Biol. Chem. 266*, 9359−9362.
17. Shimokawa, K.-i., Jia, L.-G., Shannon, J. D., and Fox, J. W. (1998) *Arch. Biochem. Biophys. 354*, 239−246.
18. Trikha, M., De Clerk, Y. A., and Markland, F. S. (1994) *Cancer Res. 54*, 4993−4998.
19. Zhou, Q., Ritter, M. R., Swenson, S. D., Argounova, S., Epstein, A. L., and Markland, F. S. (2000) *Arch. Biochem. Biophys. 375*, 278−288.
20. Nikai, T., Taniguchi, K., Komori, Y., Masuda, K., Fox, J. W., and Sugihara, H. (2000) *Arch. Biochem. Biophys. 378*, 6−15.
21. Marcinkiewicz, C., Calvete, J. J., Marcinkiewicz, M. M., Raida, M., Vijay-Kumar, S., Huang, Z., Lobb, R. R., and Niewiarowski, S. (1999) *J. Biol. Chem. 274*, 12468−12473.
22. Marcinkiewicz, C., Taooka, Y., Yokosaki, Y., Calvete, J. J., Marcinkiewicz, M. M., Lobb, R. R., Niewiarowski, S., and Sheppard, D. (2000) *J. Biol. Chem. 275*, 31930−31937.
23. Marcinkiewicz, C., Calvete, J. J., Vijay-Kumar, S., Marcinkiewicz, M. M., Raida, M., Schick, P., Lobb, R. R., and Niewiarowski, S. (1999) *Biochemistry 38*, 13302−13309.
24. Du, X., Gu, M., Weisel, M. W., Nagasawami, C., Bennet, J. S., Bowditch, R., and Ginsberg, M. H. (1993) *J. Biol. Chem. 268*, 23087−23092.
25. Bazzoni, G., Shih, D. T., Buck, C. A., and Hemler, M. E. (1995) *J. Biol. Chem. 270*, 25570−25577.
26. O'Toole, T. E., Loftus, J. C., Du, X., Glass, A., Ruggeri, Z. M., Shattil, S. J., Plow, E. F., and Ginsberg, M. H. (1990) *Cell Regul. 1*, 883−893.
27. Marcinkiewicz, C., Vijay-Kumar, S., McLane, M. A., and Niewiarowski, S. (1997) *Blood 90*, 1565−1575.
28. Gan, Z. R., Gould, R. J., Jacobs, J. W., Friedman, P. A., and Polokoff, M. A. (1988) *J. Biol. Chem. 263*, 19827−19832.
29. Wierzbicka-Patynowski, I., Niewiarowski, S., Marcinkiewicz, C., Calvete, J. J., Marcinkiewicz, M. M., and McLane, M. A. (1999) *J. Biol. Chem. 274*, 37809−37814.
30. Gasmi, A., Srairi, N., Guermazi, S., Dkhil, H., Karoui, H., and El Ayeb, M. (2001) *Biochim. Biophys. Acta 1547*, 51−56.
31. Calvete, J. J., Jurgens, M., Marcinkiewicz, C., Romero, A., Schrader, M., and Niewiarowski, S. (2000) *Biochem. J. 345*, 573−581.
32. Trikkha, M., De Clerk, Y. A., and Markland, F. S. (1994) *Cancer Res. 54*, 4993−4998.
33. Okuda, D., and Morita, T. (2001) *J. Biochem. 130*, 407−415.
34. Ritter, M. R., and Markland, F. S. (2000) *Biochem. Biophys. Res. Commun. 274*, 142−148.
35. Brando, C., Marcinkiewicz, C., Goldman, B., McLane, M. A., and Niewiarowski, S. (2000) *Biochem. Biophys. Res. Commun. 267*, 413−417.
36. Sheu, J. R., Yen, M. H., Peng, H. C., Chang, M. C., and Huang, T. F. (1995*) Eur. J. Pharmacol. 294*, 231−238.
37. Dennis, M. S., Carter, P., and Lazarus, R. A. (1993) *Proteins 15*, 312−321.
38. Lefkovitz, J., Plow, E. F., and Topol, E. J. (1995) *N. Engl. J. Med. 332*, 1553−1559.
39. Bennett, J. S. (2001) *Annu. Rev. Med. 52*, 161−184.

BI015627O